Characterization and Solid-State Properties of Processable N-Alkylated Polyanilines in the Neutral State

Wen-Yue Zheng and Kalle Levon*

Department of Chemistry and Herman F. Mark Polymer Research Institute, Polytechnic University, Brooklyn, New York 11201

Jukka Laakso and Jan-Eric Österholm

Neste Oy, Corporate R&D, SF-06150, Kulloo, Finland

Received April 14, 1994; Revised Manuscript Received August 20, 1994[⊗]

ABSTRACT: Incorporation of flexible alkyl chains into polyaniline was accomplished through an N-alkylation method with the leucoemeraldine form in order to maximize the degree of alkylation. The number of carbons varied from butyl to octadecyl, and with dodecylated samples, the degree of substitution was also controlled. The solubility in common organic solvents improved remarkably with the alkylation. The polymers displayed interesting solvatochromism and thermochromism, which result from the conformational changes induced by the interactions between the polymer and the solvent molecules and from the cooperation of disordering of the side chains and twisting in the main chain upon heating. In the solid state, the polymers form a layered structure in which the distance between the backbones depends on the length of alkyl side chain as recorded by the *d* spacing in WAXD patterns. DSC studies revealed that glass and melting transitions decreased systematically by increasing the length of substituents. With increasing side-chain length, the degree of interdigitation increases and the side chains begin to crystallize in a hexagonal packing array as determined by DSC, WAXD, and FT-IR data. The critical length *n* for side-chain crystallization is a minimum of 14 carbons, which is much larger than in the case of polyacrylates and polythiophenes, indicating the more rodlike character of polyaniline backbones. In addition, with polymers of $n \geq 16$, a mesophase transition after melting of the side-chain crystallites can be detected by optical microscopy and DSC.

Introduction

Great progress on soluble and fusible conducting polymers has been made in academic and industrial research of conducting organic materials. The development of either new conducting polymers or the improvement of known systems is essential to tailor the electronic and mechanical properties, to produce materials or devices with desired shape, thin films, and fibers, and to understand their supermolecular structure and conducting mechanism.

Among the intensive studies of conjugated polymers, polyaniline has attracted great attention recently because of its electronic, electrochemical, and optical properties, and especially because of its good environmental and thermal stability.[1,2] However, its intractability resulting from the stiffness of backbone and the hydrogen-bonding interaction between adjacent chains limits not only the industrial applications but also complete understanding of the properties of this conducting polymer. One important chemical modification has been the addition of saturated hydrocarbon alkyl or alkoxy side chains to the polymeric backbone. This approach has been successfully applied to solubilize the intractable polythiophene with alkyl groups longer than butyl.[3] In neutral state, poly(3-alkylthiophene)s (PAT) are chemically stable, sufficiently soluble in common organic solvents, and fusible far below the temperatures where thermal decomposition prevails.[4] This is in accord with the notion that the flexible side chains act much in the way of a "bound solvent" by increasing the entropy of dissolution and by screening the interaction between the main chains. Interestingly, the alkyl side chains, which have a profound influence on the microstructure of the comblike polymer, introduce some unique properties such as solvatochromic behavior and reversible thermochromic transition between the low- and high-temperature solid-state phases.[5] The rodlike character of the main chains coupled with the presence of the aliphatic side chains creates the semirigid polymer systems. These polymers exhibit interesting thermal and morphological properties in the bulk state. The possibilities of the formation of discrete crystallinity of the paraffin side chains and the appearance of a thermotropic liquid crystal state in this type of polymers have been studied extensively.[6,7] Furthermore, most of these systems exhibit the ability to form well-defined layered structures in three dimensions. The rigid main chains are packed into the platelike layers, and the alkyl side chains are arranged between the layers forming paraffinic crystallites.[8] For conducting polymers featured with long conjugated structure, the incorporation of substituents into conducting polymers may affect the conjugation along the polymeric backbone and may bring up the steric hindrance and relatively enlarge electronic band gaps. With regard to conduction, the nitrogen plays a key role in the electronic transportation, in which the molecular orbital and lone pair electrons are involved. Therefore, the study of polyanilines with different substitutions on the nitrogen atom should be helpful to understand the basic chemistry and physics of this polymer.

From the viewpoint of the aniline structure, there are three sites that can be modified including ortho and meta positions in the aromatic ring and one on the amine group. In past studies, the polymers have been obtained from corresponding substituted monomers. *N*-Alkyl-substituted[9] or alkyl-ring-substituted[10,11] polyanilines were always prepared as the low molecular

* To whom the correspondence should be sent.

[⊗] Abstract published in *Advance ACS Abstracts,* November 1, 1994.

0024-9297/94/2227-7754$04.50/0

weight species due to the steric effect of the side group in the polymerization of the substituted monomers, which is an inherent limitation in the process.

In our work, the substitution was carried out through N-alkylation of the amine group in the completely reduced polyaniline leucoemeraldine base (PANi-LB). We wanted to start the alkylation from the LB form in order to maximize the degree of alkylation. The replacement reaction at the N position via polyanion is formed by H elimination of the aromatic secondary amine as shown in Schemes 1 and 2.[12] This method has been used by Takayanagi and Katayose[13] and other groups[14] for substituting of alkyl side chains, ionic side chains, and polymeric groups onto the aromatic polyamide backbone. Such a modification would result in processable conducting species with high molecular weight. The products are easily cast to be strong free-standing films with metallic color.

In this paper, we report a comprehensive study of the N-alkylated polyanilines with an increasing length of the side chain from 4 to 18 carbons and controlled extent of substitution in the modification. Furthermore, a fully N-alkylated polyaniline is prepared via oxidative polymerization from the corresponding monomer. Although the solution properties of alkylated polyanilines have been reported before,[9] we present the solution behavior of the N-alkylated polyanilines because the alkylation was done on the LB form, and thus, the degree of alkylation was done in a systematic control. The main emphasis in our study is to relate the structural characteristics to the solid-state properties. Through the study of these polyanilines, our objective is to investigate how a fine control of the polymer structure and design of conjugated polymers with tunable physical properties can be achieved by the introduction of alkyl side substituents onto the main chains.

Scheme 1

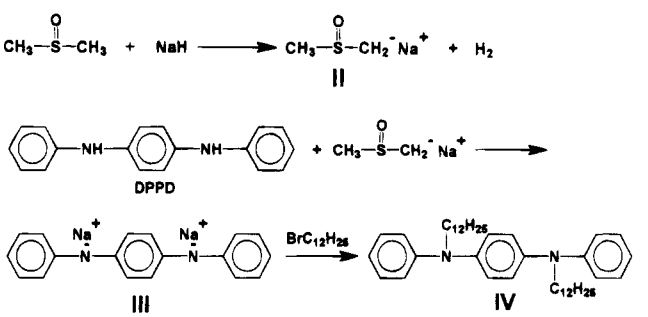

Scheme 2

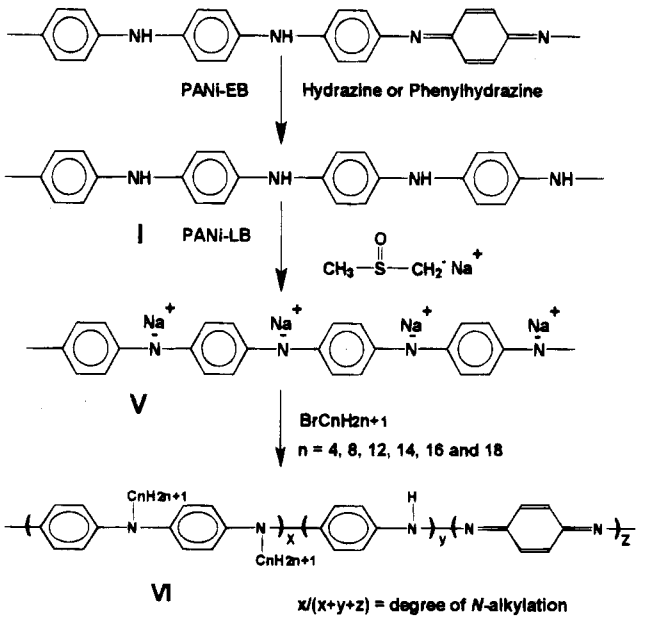

Experimental Section

1. Materials. Dimethylsulfoxide (DMSO) and 1-methyl-2-pyrrolidinone (NMP) were anhydrous grade from Aldrich. Alkyl bromide, NaH, $CHCl_3$, tetrahydrofuran (THF), and deuterated solvents used in NMR measurements were commercial grades from Aldrich and used without further purification. *N*-*n*-Butylaniline and *N*-*n*-dodecylaniline were purchased from American Tokyo Kasei. Reagent grade protonic acids, ammonium hydroxide, and amonium persufate from Aldrich were also used as received. Polyaniline with M_w = 92 200, M_w/M_n = 4.2 was synthesized and supplied by Corporate R&D, Neste Oy, Finland.

2. Methods. N-Alkylation Reduction of Emeraldine Base. The starting material, leucoemeraldine (**I**), the completely reduced form of polyaniline, was prepared by treating polyaniline emeraldine base (PANi-EB) powder in methanol with hydrazine or phenylhydrazine for 48 h. The collected gray-white powder was extracted by THF to remove excess reducing agent and the small molecular weight species.

Synthesis of *N,N'*-Bisalkyl-*N,N'*-diphenyl-1,4-phenylenediamine. A 150 mL aliquot of DMSO and 0.65 g (0.0269 mol) of NaH were added to a 250 mL nitrogen-flushed reaction flask equipped with magnetic stirring. The mixture was heated to 50–60 °C and stirred until NaH was dissolved. A solution of methylsulfinyl carbanion (**II**) in DMSO was obtained as described in detail by Takayanagi and Katayose.[13]

A 2.80 g sample of Gray powder *N,N'*-diphenyl-1,4-phenylenediamine (DPPD; 0.0215 mol) was put in a solution (**II**) in methyl sulfoxide at 60 °C, and the metalation reaction as described in Scheme 2 was conducted for 4 h. Then 5.36 g of *n*-dodecyl bromide (0.0215 mol) was dropped in the reaction flask with the brown DPPD anion solution (**III**) at room temperature. After 4 h, a yellow precipitate developed, and it was filtered and washed with a large amount of water. The blue powder was isolated by pouring a solution of this precipitate in propanol into 0.5 M aqueous HCl. The blue precipitate was washed with MeOH, and the product (**IV**) salt was extracted into MeOH, whereas the starting material salt remained insoluble. The blue product (**IV**) salt was then neutralized by $NH_3 \cdot H_2O$ and washed by water extensively. The product was finally recrystallized from the mixture solvent of chloroform and heptane. Yield, 4.32 g (53%). Elemental Anal. Found: C, 83.9; N, 4.6; H, 10.3. Calcd: C, 84.6; N, 4.7; H, 10.7.

Preparation of N-Alkylated Polyaniline. A 2.0 g sample of polyaniline leucoemeraldine (PANi-LB; 0.0215 mol) was added to sodium methylsulfinyl carbanion (**II**) solution at 60 °C and the metalation reaction was contined for 4 h. The resulting anion solution (**V**) was dark yellow, viscous, moisture sensitive, and did not contain solid PANi-LB residue. This viscous solution was cooled to 40 °C and 5.36 g (0.0215 mol) of *n*-dodecyl bromide was dropped in. The viscosity of the solution dropped gradually, and the color turned finally blue. The reaction was continued for 16 h and a blue sticky precipitate developed. The precipitate was extensively washed with methanol, water, and acetone alternately to remove all unreacted species. A green fiberlike material was obtained by pouring the solution of the precipitate in THF to 0.5 M aqueous HCl; the resultant mixture was washed with water and acetone and was then neutralized in $NH_3 \cdot H_2O$. A total of 5.2 g of the blue product (**VI**) was collected with a yield of ~70%. The density of the alkyl substitution and size of the alkyl chains were controlled by varying the amount of the added alkyl bromide and using alkyl bromide with 4–18 carbons separately.

Chemical Polymerization of Poly(*N*-Alkylaniline). Water-soluble complex salt **VII** was prepared by mixing 0.02 mol of *N*-dodecylaniline with methanesulfonic acid. Polymer was synthesized by chemical oxidation of the monomer (*N*-dode-

cylaniline) in 1.0 M aqueous CH_3SO_3H. After a dropwise addition of 0.03 mol of ammonium persulfate in 1.0 M aqueous CH_3SO_3H to the monomer solution, the reacting mixture was stirred for another 4 h to complete polymerization. The polymer was collected and washed with water and methanol. The black sticky product (**VIII**) obtained was in a doped state and was then neutralized by using $NH_3{\cdot}H_2O$. The brown product with yields up to 94% was dried under vacuum oven. Poly(*N*-butylaniline) was also prepared in the same way to be a reference in FT-IR measurements.

3. Characterization. Elemental analyses were operated by the Analytical Laboratory, Neste Oy. ^1H and ^{13}C NMR spectra for all the model compounds and polymers were measured in deuterated chloroform solutions with GE GN300-MHz FT-NMR spectrometer using TMS as the internal reference. ^{13}C NMR spectra were obtained with broad-band proton decoupling. Infrared spectra were recorded with a Perkin-Elmer 1600 FT-IR spectrometer connected to a PC computer with the Spectrum Calculation program. Spectra were taken of neat films on KBr plates. UV spectra were obtained on a Varian 100 UV–visible spectrometer. Spectral grades of $CHCl_3$, NMP, and THF were used as the solvents for the model compounds and the polymers. Thin films of polymers were prepared on a flat quartz surface from dilute solution for solid state measurements.

The thermal transitions of the polymers were determined by differential scanning calorimeter on a Perkin-Elmer TAS7 DSC with a cooling unit. The instrument was calibrated with indium (mp, 156 °C); 10–15 mg was weighed for each sample. The scan rates ranging from 5 to 20 °C/min were used in cooling and heating cycles, and the transition temperature was reproducible up to 2 °C. The enthalpies and mediated points of transitions were calculated by digitally integrating the area of the endothermic and exothermic peaks and expressing these values in units of joules per gram.

Thermal stability of the polymers was tested by thermogravimetric analysis (TGA) using a Du Pont Instrument 1090 thermal analyzer with a 951 thermogravimetric analyzer. The tests were carried out with nitrogen gas purge. The weight of a sample used was ~10 g.

Microscopic observation was performed with a Nikon microscope equipped with a hot stage. A Philips APD 3720 X-ray generator was used for the WAXD experiments. The point focus beam was monochromatized to Cu Kα with a graphite crystal. X-ray diffraction data were recorded by a diffractometer. The X-ray source, a XRG 3100 generator, utilized a Cu Kα target ($1_{K\alpha}$ = 1.5406 Å) with generator settings of 40 kV and 20 mA. The 2θ step size for each individual data collection point was set into 0.04°, and the interval time on every point was limited to 50 s.

Results and Discussion

A. Synthesis and Modification. 1. Model Compound Study. To investigate the activity of the protonated nitrogen atoms inherent in the benzenoid unit of polyaniline, a simple three-ring oligomer DPPD was studied as a model for PANi in the modification reaction. DPPD is a dimer of aniline with a phenyl ring as an end cap. This compound has been commonly used as an example for the study of structure, doping process, and optical properties of PANi in various states.[15] The N-alkylation procedure is illustrated in Scheme 1. The anion of DPPD was obtained in DMSO with NaH. After deprotonation for formation of the anion, an alkyl bromide reagent for introduction of the alkyl group was added to give product **IV**. The extent of N-alkylation on DPPD was calculated on the basis of the elemental analysis data and the integrated values in ^1H NMR spectra suggesting the substitution of up to 100% of the nitrogen atoms as presented in the Experimental Section.

The ^{13}C chemical shifts for DPPD and its derivatives are shown in Figure 1. The aromatic peak assignments

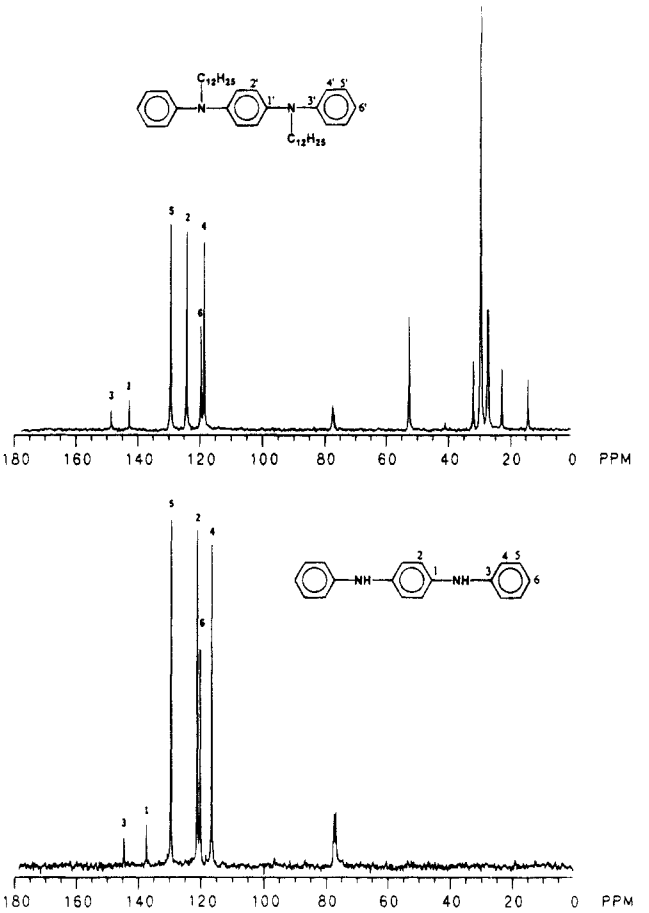

Figure 1. ^{13}C NMR or DPPD and N-alkylated DPPD in $CDCl_3$.

for DPPD and the derivatives (DPPD-12) were done with the help of estimation of the incremental shifts from benzene of the aromatic carbons of monosubstituted benzene rings. The farthest upfield aromatic carbons (1 and 3) are shifted significantly upfield by alkyl substitution at the nitrogen. This shift is due to the inductive effect of the hydrocarbon substituent, increasing the electron density on the nitrogen, the N–C bond order, and the electron density of the ring. The small change of other resonances (2 and 4) in chemical shifts resulted from the slight change of carbon environments, and 5 and 6 remained unchanged. Observation of the shifts aids in the assignment of the carbon peaks in N-alkylated polyanilines as will be discussed below. All the resonances in the high field are assigned to the aliphatic carbons. Inspection of the chemical shifts for the dodecyl group in the DPPD derivative also allows assignment of alkyl resonances in the polymer products. The farthest upfield peak at 14.5 ppm is assigned to the terminal methyl carbon, the one at 52.5 ppm to the carbon next to the nitrogen, and the rest of the carbon resonances in the dodecyl chain are at 31.9, 29.7, 27.4, 27.1, and 22.7 ppm. Therefore, DPPD and its derivative were used not only to verify the proposed reaction for polyaniline but also especially to assist in the structural assignment of modified polymers.

The infrared spectrum of N-alkylated DPPD shows the complete disappearance of a stretching band at 3300 cm^{-1} for the N–H bond, which indicates that the hydrogens on nitrogens have been substituted. The N–C stretch vibration and C–H stretch vibration in the middle ring are also greatly influenced by the alkylation.

Table 1. Degree of N-Alkylation and Instrinsic Viscosity of Polyaniline Derivatives with Various Side Chain Substituents

polymer	n of the side chain	% alkylation EA[a]	FT-IR	^{1}H NMR	$[\eta]$,[b] dL/g
PAN-EB	0				0.74
PANi-4	4	83.3	78.3	83.9	0.54
PANi-8	8	74.5	73.2	80.0	0.38
PANi-12d	12	21.6	24.0		0.52[c]
PANi-12c	12	37.9	40.2	50.3	0.45
PANi-12b	12	59.0	61.1	65.8	0.31
PANi-12a	12	76.8	80.5	81.7	0.26
PDAN	12	100	100	100	0.16
PANi-14	14		76.3	80.9	0.21
PANi-16	16	72.5	75.7	78.3	0.17
PANi-18	18	67.2	69.1	70.5	0.16

[a] EA, from the data of elemental analysis. [b] Viscosity of the polymers was determined in $CHCl_3$ solution. [c] Viscosity of the polymers was determined in NMP solution.

In addition, the appearance of C−H or C−C vibration correlated to the aliphatic group is additional evidence of the success of the N-alkylation process.

2. N-Alkylation of PANi. PANi-LB, the completely reduced form of polyaniline composed of only aromatic secondary amines along the backbone was used to prepare the N-alkylated derivative in order to maximize the degree of substitution and to avoid any side reactions. The reduction of the emeraldine base can be conveniently done as in described in Scheme 2. The dramatic depression of absorption intensity at 1600 cm^{-1} in the FT-IR spectrum of PANi-LB in contrast to that of emeraldine (PANi-EB) indicates the structural conversion from the quinoid to the benzenoid form. The absorption at 630 nm—a transition in the UV−visible spectrum related to the quinoid form, almost totally disappears, and only the $\pi \rightarrow \pi^*$ benzenoid absorption exists at 320 nm as shown later in Table 3. This also indicates the elimination of the oxidation state in polyaniline.

One advantage of the polymer modification is that low molecular weight species via chemical polymerization of *N*-alkylaniline can be avoided. Direct N-substitution was adopted earlier for PPTA and PBI derivatizations to prepare soluble materials.[13,14] We utilized this method to prepare alkylated derivatives of polyaniline under moderate conditions. Another priority of this approach is the ability to control the stoichiometry among NaH, PANi-LB, and alkyl bromide to make the products at the desired levels of partial N-alkylation. A significant observation noted during modification was that PANi-LB dissolved well in DMSO with NaH. The viscosity of this yellow solution decreased gradually after the alkyl bromide was added.[16] A blue precipitate developed at the end of the substitution reaction with indication of autoxidation of the product by oxygen. The precipitation impedes the hydrogens on the nitrogen atoms from being completely replaced by alkyl groups. On the other hand, a complete alkylation may not be a necessity to obtain a processable polymer. The degrees of alkylation for the various modified polyanilines are summarized in Table 1. Because of the good solubility, the purification of the products was achieved through dissolution in THF or dioxane, reprecipitation into aqueous protonic acids followed by intensive washing with methanol and acetone to remove all unreacted substances, and finally neutralization in $NH_3{\cdot}H_2O$.

3. Oxidative Polymerization of *N*-Alkylanilines. Of particular interest is the synthesis and characterization of the polymer where the alkyl groups are attached to all nitrogen atoms so that their properties and structures can be compared with those of the polymers with partial alkylation. For this purpose, poly(*N*-dodecylaniline) and poly(*N*-butylaniline) were synthesized via chemical polymerization. The water-soluble complex salts were made prior to polymerization to prepare the polymers with high molecular weight because aniline bearing a long hydrocarbon chain could not dissolve in aqueous reaction media. The characterization of these fully alkylated polymers and the comparison with partially alkylated ones are presented below in regard to the characterization methods.

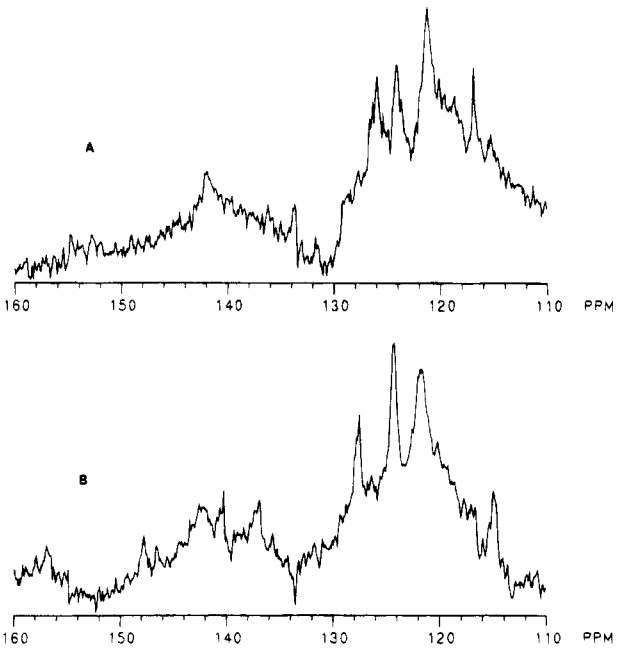

Figure 2. Aromatic regions of the ^{13}C NMR spectra for PDAN (A) and PANi-12b (B) in $CDCl_3$.

B. Structural Characterization of the N-Alkylated Polymers. 1. NMR Spectroscopy. The proposed structures of the alkylated polymers and synthesized polymers were confirmed by FT-IR, ^{1}H and ^{13}C NMR, and UV−visible spectroscopies. The ^{1}H NMR spectra for poly(*N*-dodecylaniline) (PDAN) and for N-dodecylated polyaniline with different degrees of alkylation in $CDCl_3$ show the peaks with the same chemical shifts but different intensities of the aromatic and aliphatic resonances due to the various alkylation levels. The broad peak around 6.8 ppm corresponds to the aromatic protons, while the peaks at 3.70, 1.64, 1.37, and 0.95 ppm are correlated to the protons of the methylene C_2, C_{3-11} and to the end methyl C_{12}, respectively. The intensity ratio of the aromatic and aliphatic peaks was used for the calculation of the degree of alkylation as tabulated in Table 1. The protons of C_1, directly bonded to nitrogen, appear as a small peak at ~3.7 ppm overlapped by a peak at 3.5 ppm attributed to the residue water in the samples. Another feature in the spectra for N-alkylated polymer is the very weak peak of N−H amine hydrogen resonance near 5 ppm.

Great efforts have been made to investigate the details of the chemical structure of polyaniline by high-resolution ^{13}C NMR spectra in solution state.[17,18] In this work, ^{13}C NMR spectra were obtained at 25 °C in DMSO-*d* for the emeraldine base and in $CDCl_3$ for soluble alkylated polyanilines. Here, a partially substituted polymer PANi-12b (A) and fully substituted polymer PDAN (B) are shown as a comparison in Figure 2. The spectrum of the pristine emeraldine base obtained in

DMSO-*d* is exactly the same as that reported in the literature.[17] The most informative region is the aromatic resonances in the downfield as shown in Figure 2. It is obvious that there are three groups of peaks located at 115–127, 136–148, and 156 ppm, respectively. Due to the poor resolution in ^{13}C NMR results and inconsistent assignments for conjugated polyaniline in three oxidative states in the past, the analysis of these spectra becomes difficult. It is believed that the resonance at 157.0 ppm in PANi-12b results from the unprotonated carbons in the quinoid ring and does not exist in PDAN as expected.[18] At least four resonance peaks overlapping from 140 to 148 ppm, compared to the two main peaks at 141.5 ppm and 144.0 ppm in PANi-EB, can assigned to unprotonated carbons in the benzenoid unit. On the basis of the study of the alkylated model compound, the absorbances in DPPD-12 at 143.0 and 147.9 ppm are upshifted forms of carbons 1 and 3 in Figure 1, respectively. It can also be assumed that the new resonances arise from the change of chemical environment brought about by the electron donor-alkyl group. The peak at 136 ppm attributed to proton-bonded carbons in the quinoid ring does still exist in PANi-12b with less intensity.

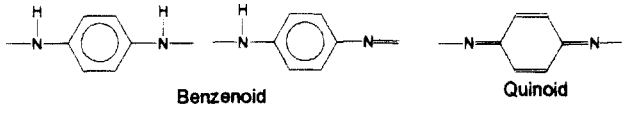

One prominent peak centered at 142 ppm belonging to the unprotonated carbons in PDAN is in accord with the proposed simple structure of fully alkylated repeat units in which carbons 1 and 3 have similar electronic environments in contrast to DPPD. At the higher field, PANi-12b and PDAN present similar sets of the resonance peaks with identical chemical shifts from 114 to 128 ppm. These peaks are assigned to the protonated carbons in benzenoid rings—highest concentration of carbons in the polymers. The whole resonance group seems to be upshifted from that in PANi-EB. A similar upshift in this region with alkylation was observed with the model compound. The complexity of aromatic resonances between 115 and 130 nm indicates that the chemical surrounding is not as uniform as expected.

2. FT-IR Spectroscopy. Major changes are observed in the FT-IR spectra as illustrated in Figure 3, where leucoemeraldine and N-alkylated polyanilines at various alkylation levels are presented. The characteristic aliphatic CH_2 stretching vibration bands at 3000–2800 cm^{-1} increase in intensity with the percentage of N-alkylation. The positions of the peaks around 1600 cm^{-1} for the quinoid ring and 1500 cm^{-1} for the benzenoid ring[19] have been upshifted gradually with an increase in the extent of alkyl substitution. For instance, the peaks (Q/B) move from PANi-LB at 1589/1495 cm^{-1} to PANi-12d, -12c, -12b, and -12a at 1595/1501, 1595/1501, 1597/1503, and 1599/1504 cm^{-1}, respectively, and ultimately to PDAN at 1607/1504 cm^{-1}.

Similar to the other CH_2 bands, a medium-intensity absorption near 1460 cm^{-1} increases with the percentage of alkylation. A group of infrared bands in the 1400–1300 cm^{-1} range is usually assigned to sequences of gauche conformation of the alkyl chain. For example, *gtg'*(*kink*)(*t-trans*, *g-gauche*) vibration is usually at ~1370 cm^{-1}, which downshifts from that in PANi-12d with least alkylation at 1376 cm^{-1} to that in PANi-12c, -12b, and -12a at 1372, 1372, and 1367 cm^{-1} and ultimately to completely alkylated PDAN at 1362 cm^{-1} with most intense absorption. Similarly, another weak peak at 1282 cm^{-1} in the leucoemeraldine, and 1301 cm^{-1} in the emeraldine base, which is due to mixed vibrations of the C–H bend and the C–N stretch shows the same shift tendency to 1306 cm^{-1} by 5 cm^{-1} in PANi-12a and PDAN. The peak near 1180 cm^{-1} is a characteristic of the =N– vibration, still sharp in alkylated PANi's, indicating the presence of the quinoid structure. This absorbance is heavily influenced by the substituent on the nitrogen site and shifts to higher wavenumbers. The CH_2 rocking bands at 730 cm^{-1}, indicating the *trans* sequence of the alkyl chain, are intense in long alkyl-substituted and heavily substituted polymers. From all absorbances related to the vibrations from the aliphatic groups, it is found that the alkyl side chains become more ordered with the intense of the alkylation level and the length of the alkyl chains; this will be discussed in the following sections. In other aspects, the shifts of the absorption bands from aromatic vibration indicate that the structural and geometrical features have been dramatically affected by the N-substitution.

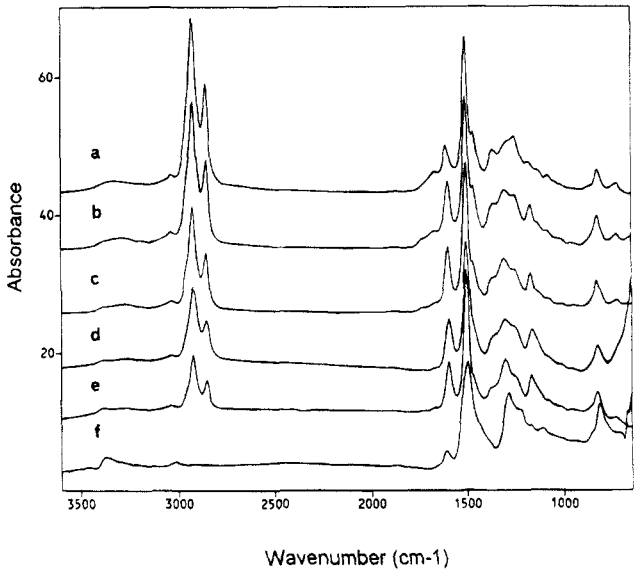

Figure 3. FT-IR absorption spectra of PDAN (a), PANi-12a (b), PANi-12b (c), PANi-12c (d), PANi-12d (e), and parent leucoemeraldine (f).

The compositions can be quantitatively determined from the IR spectra because poly(*N*-dodecylaniline) and poly(*N*-butylaniline) can serve as the reliable references. The relative integrated areas of the absorbances at 3000–2800 cm^{-1} to the sum of the area of 1600 and 1500 cm^{-1} can be used to estimate the percentage of amine replaced by alkyl substituent.[20] The relationship between DS and $A_{2900}/(A_{1600} + A_{1500})$ can be expressed as

$$\text{DS (in mol \%)} = 5.2n(A_{2900}/(A_{1600} + A_{1500})) + 1.4$$

where n is the carbon number of the alkyl chain. This relationship was used for calculation of the degree of alkylation as tabulated in Table 1.

3. Solubility, Viscosity, and Molecular Weight. Improvement of the solubility of stiff polymers by incorporation of the alkyl side chain in the polymer backbone has been reported extensively.[3,4,12–15] For instance, for poly(3-alkylthiophene), the solubility and fusibility have been achieved through addition of relatively long, flexible hydrocarbon side groups without significantly changing the π-electronic structure. The

Table 2. Improved Solubility[a] of N-Alkylated Polyanilines in Various Solvents

polymer	H_2SO_4(conc)	NMP	DMF	pyridine	dioxane	THF	$CHCl_3$	toluene	hexane
PAN-EB	++	++	+	+	−	−	−	−	−
PANi-4	+	++	+	+	−	−	−	+−	−
PANi-8	+	+	+	++	++	++	++	+	−
PANi-12d	+	++	+	+	+	+	−	−	−
PANi-12c	+	+	+	++	++	++	++	++	−
PANi-12b	−	+	+	+	++	++	++	++	−
PANi-12a	−	+	+	+	++	++	++	++	+
PDAN	−	+	+	+	++	++	++	+	−
PANi-14	−	−	−	+	++	++	++	++	++
PANi-16	−	−	−	+	++	++	++	++	++
PANi-18	−	−	−	+	++	++	++	++	++

[a] Key: ++, well soluble; +, partially soluble; −, slightly soluble or insoluble.

influence of alkylation on similar properties of polyaniline was studied in our approach. The qualitative solubility and intrinsic viscosity values of the N-substituted polymers are summarized in Tables 1 and 2. In contrast to the unsubstituted polyaniline emeraldine base (PANi-EB), and N-alkylated polymers bearing more than eight carbons and with more than 38% of alkylated units already exhibit sufficient solubilities in chloroform, toluene, THF, and other common organic solvents. Polyanilines bearing longer side chains, such as PANi-16, and PANi-18, may even be dissolved in hexane and methylene chloride. It agrees with the concept that the side chains act as "bound solvents" in the class of rigid polymers with flexible side chains. In addition, the increase of solubility may be owing to a lowering of the stiffness of polymeric chains as discussed later. However, polar solvents such as NMP, DMSO, and DMF are no longer good solvents for these heavily substituted polyanilines. It is usually believed that the strong hydrogen-bonding interaction contributes to the dissolution of polyaniline emeraldine base in NMP, DMSO, and *m*-cresol.[1] Now as a consequence of the "paraffin phase" formed by the alkyl side chains, these substituted polyanilines lack some of the functional groups that can participate in hydrogen bonding and solvation, thereby diminishing their solubility in the strong polar solvents. The discrepancy in the solubility of the alkylated polyaniline depends not only on the presence of the side chain with a certain concentration but also on the size of the pendant side chain. Once a solution is formed, it is stable at ambient conditions up to the concentration of 2.5 g/100 mL for months without precipitation and without a color change.

The inherent viscosity values which were measured for the polymers in $CHCl_3$ or NMP at 25 °C lie in the range of 0.74−0.16 dL/g as shown in Table 1. The data show that the intrinsic viscosities of the N-alkylated PANi solutions in $CHCl_3$ decrease drastically as the fraction of alkylated amine units increases and the size of alkyl side chain increases. In our experiments, it has been shown that during the alkylation procedure the molecular weights of the samples decrease. The PANi-LB polyanion in DMSO was precipitated in aquous HCl media and then neutralized to PANi-EB. This sample had an intrinsic viscosity in $CHCl_3$ of 0.63 dL/g compared to 0.74 dL/g for the starting PANi-EB. The change of molecular weight may occur during the reduction process of polyaniline from the emeraldine form to the leucoemeraldine form by phenylhydrazine or hydrazine, as studied by Wei et al.[21] or during the deprotonation reaction of leucoemeraldine in DMSO by NaH.

In the absence of reliable measurements of the radius of gyration by light scattering, the intrinsic viscosity $[\eta]$ may be used to estimate the stiffness of the polymer chain in the selected solvent. The dependence of $[\eta]$ on the fraction of alkylated amine units as well as the size of the alkyl side chain is summarized in Table 1. The flexibility seems to increase both with increasing degree of alkylation and increasing length of the side chains (at least from butyl to dodecyl substitution). It will be shown with UV−visible data in Table 3 that the fraction of quinoid forms along the polyaniline backbone inducing the stiffness of the backbone decreases and the length of conjugation decreases due to the partial alkylation.

4. Optical Properties of N-Alkylated Polyanilines. Optical properties have played a key role in the elucidation of the basic electronic structure in the conducting polymers. Significant changes in their optical absorption are always accompanied with changes in chemical structure, quality of the solvents, temperature, and extent of doping. The absorption changes caused by the solvent and temperature are called solvatochromism and thermochromism, respectively.[22] The influence of alkylation on the chromic effects have been extensively studied for poly(3-alkylthiophene).[23] PANi-EB has two classic absorptions;[1] one at 625 nm (~2 eV) is assigned to the excitation from the highest occupied molecular orbital (HOMO, π_b) of the three-ring benzenoid part of the system to the lowest unoccupied molecular orbital (LUMO, π_q) of the localized quinoid ring with the two surrounding imine nitrogens. The absorption at 320 nm (~4 eV) is attributed to the $\pi \rightarrow \pi^*$ transition associated with π electrons of the benzene ring delocalized on nitrogen atoms of the amine groups. The energy level diagram for polyaniline has been presented in literature.[24] All of the spectra of the neutral polymers dissolved in NMP, except leucoemeraldine, consist of two absorption peaks as shown in Table 3. The absorptions show a significant bathochromatic shift from the 330 nm of PANi-EB, to the 315 nm of PANi-12a, and finally to the 305 nm of PDAN. Thus the absorption is sensitive to the degree of substitution, but is independent of the size of substituent as shown in Table 4. The hypsochromic shift in the absorption near 600 nm is a trend similar to that in the $\pi \rightarrow \pi^*$ transition. The red shift decreases with increasing length of the side chain, but an objective comparison is difficult because the shift is also sensitive to the degree of substitution. It is known that the relative intensity of the absorption at 600 nm to the absorption at 300 nm is proportional to the composition of quinoid units and benzenoid units along polymer backbone. It may be used for a quantitative estimation of the level of N-alkylation as the data shown in the third columns of Tables 3 and 4. The existence of relatively weak absorption near 600 nm in PDAN suggests the presence

of certain amount of oxidized units even in this completely alkylated sample as presented in the following:

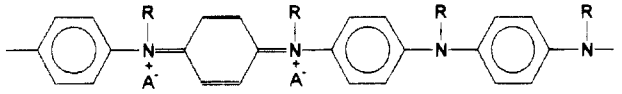

The presence of the oxidized quinoid forms in PDAN is also evident from the greater relative intensity of the 1600 cm^{-1} peak vs the 1500 cm^{-1} peak in FT-IR spectra as compared to that in leucoemeraldine and also from the multiple resonance peaks around 110–135 ppm in ^{13}C NMR spectra. Barbero et al. have also determined the quinoid formation in the neutralized polymers which were polymerized from the fully alkylated monomers and emphasized chemical structure affected by the electron-donating character of the alkyl group.[25]

The absorptions for solution casting films of the alkylated polymers are compared in the forth columns of Tables 3 and 4. The N-alkylated polyaniline solution with the highest degree of alkylation in $CHCl_3$ or THF can be processed into good free-standing thin films. The spectral characteristics of the solid film are not identical to those of the NMP solutions, though the chemical structure is unchanged after dissolution of the polymers. The complicated situation of optical absorption for these polyanilines in the solid state will be discussed later under Solid-State Properties.

The values in Table 3 indicate clearly the increasing flexibility (red shift from 635 to 602 nm) with degree of alkylation, but on the other hand when comparing the data in Table 4 for the solvent-cast samples, a similar trend is not obvious. It is known that the ionization potential, band gap, and band width of polyaniline are affected by the torsion angles between adjacent rings. According to the theoretical and experimental studies,[1,2] one model is suggested to describe a noncoplanar conformation for partially alkylated polyaniline backbone:

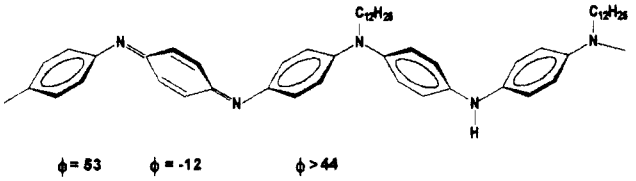

Therefore, the alkyl group on the N sites in the backbone can be expected to increase the torsional angle ϕ between adjacent rings because of the steric hindrance. This will cause the degree of orbital overlap between the phenyl π electrons and the nitrogen lone pairs to decrease. This will further decrease the extent of π conjugation and increase the energy level of LUMO π_q. However, another factor should be considered, which is the electronic effects of the hydrocarbons. The electron-donating character of the alkyl group increases the density of the electrons on the N atoms, enhancing the dipole moment. This would assist the formation of conjugated structure and lower π_q. According to the red shift in the UV absorption spectrum, the electronic effect of the alkyl substituent ultimately becomes dominant.[26]

This observation in the optical absorption spectrum is consistent with the fact that IR absorbances associated with quinoid diimine and benzenoid diamine structures are changed by N substitution as discussed earlier. Combining these IR results with the UV wavelengths in Tables 3 and 4, the conclusion can be easily made that the overall decrease of the conjugation length is directly correlated to the torsional angle twisted by the bulk substituting groups.

Table 3. UV–Visible Absorptions of Polyanilines and Their Derivatives with Different Degrees of N-Dodecylation in NMP Solution and Solid State

	wavelength, nm (in NMP solution)		ratio of intensity,	wavelength, nm (in
polymers	A1	A2	I_{A1}/I_{A2}	solid state) A1
PANi-EB	630	330	0.90	635
PANi-LB		335		
PANi-12d	620	328	0.73	630
PANi-12c	618	325	0.45	626
PANi-12b	614	320	0.38	622
PANi-12a	610	315	0.32	618
PDAN	585	305	0.24	602

Table 4. UV–Visible Absorptions of Model Compounds and Polyanilines N-Alkylated by Various Side Chain Substituents in Chloroform Solutions and in Solid State

	wavelength, nm (in $CHCl_3$ solution)		ratio of intensity,	wavelength, nm (in
polymers and model compds	A1	A2	I_{A1}/I_{A2}	solid state) A1
PANi-4	610	321	0.24	626
PANi-8	608	309	0.25	622
PANi-12a	606	308	0.26	618
PDAN	585	305	0.14	602
PANi-14	604	308	0.29	620
PANi-16	598	307	0.32	616
PANi-18	600	308	0.35	620
DPPD		307		
DPPD-12		300		

The changes in the optical absorption are important for understanding of the conformation changed by the interaction between the solute and the solvent molecules and by thermal treatment. Figure 4 shows the UV spectra of the PANi-12b in various solvents. In the dilute solutions with concentrations around 10^{-3}–10^{-4} M, the blue solutions of PANi-12b in NMP and in DMF shift to purple solutions in dioxane and in toluene. Similar solvatochromism was observed for PDAN as summarized in Table 5 and for PANi-EB in the literature.[27] Qualitatively, the phenomenon can be explained by the electron transfer between the solvent molecules and the imine and amine units of the solvated polymer. This interaction increases the electron density of the imine nitrogen, enhancing the dipole moment directed toward the nitrogen atom and consequently lowering the energy of the ground-state π_b, HOMO. Comparison of the data from PANi-EB, PANi-12b, and PDAN solution, shows the solvatochromic effect is more significant in PANi-EB than PANi-12b and PDAN because the electron density on the nitrogen of the substituted amine has been enhanced by the electron-donating feature of the alkyl group. This increase of electron density on the benzenoid ring extends over the next quinoid ring and two neighboring imine nitrogen atoms, so that less absorption is affected by the nature of solvents as expected.[27]

The optical absorptions of the PANi-12b solution are also varied by the change of the ratio of dioxane to NMP in the mixtures of these solvents. Similar solvatochromism was observed when NMP was gradually added to a solution of PANi-12b in dioxane, in which the color changed gradually from purple to blue. These results can also be explained by the interaction of the polymer backbone in the different solvent environments as noted above. This solvatochromism brought out by the solvent mixtures has been reported by MacDiarmid et al.[28] for sulfonated polyaniline emeraldine base

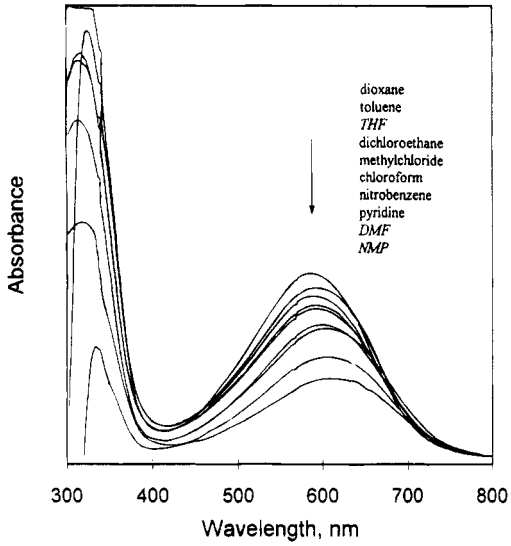

Figure 4. UV–visible absorption spectra of PANi-12b solutions in different solvents.

Table 5. Solvatochromic Phenomena of N-Alkylated Polyanilines

	wavelength, nm			
	PANi-12b		PDAN	
solvents	A1	A2	A1	A2
dioxane	585		580	
toluene	588		576	
THF	590		585	
dichloroethane	592	314		
methyl chloride	592	314	572	304
chloroform	600	318	580	306
nitrobenzene	606			
pyridine	608		598	
DMF	610	320	600	312
NMP	614	320	604	314

(PANi-EB) where the blue shift of ~2 eV optical absorption occurred with gradual addition of NMP into a water solution.

Yoshino et al. concluded that, in the solvatochromic behavior of N-alkylated polyanilines, the solvent donor–polymer chain acceptor interaction plays the dominant role.[29] The fact that the shift of the absorption maxima did not depend on the dielectric constant of the solvent resulted in the conclusion that dipole interactions are not prevailing between the solvent and polymer. They also stated that the conformational changes in the side chain do not have a major role in the solvatochromism though they are essential to solubility. All these results, and especially the use of Taft's β value for the hydrogen bond acceptor ability, would be indicative of a low degree of substitution in EB (which is known for its strong interchain hydrogen-bonding capabilities). Our results show that dipole interactions do have importance since the absorption shift is linearly dependent on the dielectric constant of the solvent in our case. In addition, we do feel that the decrease in the conjugation length is influenced by the conformational changes in the side group but agree with Yoshino's opinion that it is not as dominant as in poly(alkylthiophene).

The characterization of the N-alkylated polymers in solution state by optical spectroscopy has evidenced that the control of the degree of alkylation and the variation in the length of the side chain offers a great opportunity to modify the interaction characteristics of polyaniline, and it is interesting to evaluate similar effects in solid state.

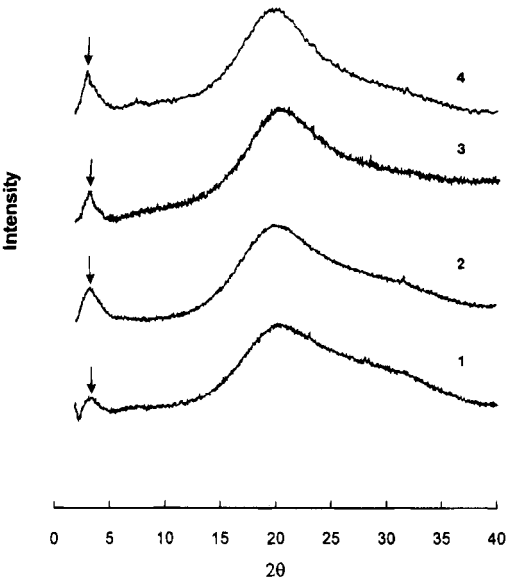

Figure 5. X-ray diffraction patterns for (1) PANi-12b, (2) PANi-12a, (3) PDAN, and (4) PANi-14 films cast from THF solution.

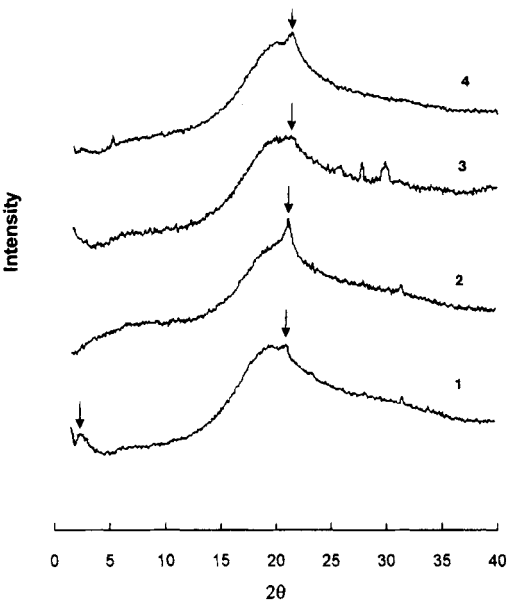

Figure 6. X-ray diffraction patterns for (1) PANi-16, (2) PANi-18 films cast from THF solution, (3) quenched PANi-18 solution-casting film, and (4) the former sample annealed at room temperature for 1 week.

C. Solid-State Properties. 1. X-ray Diffraction and Crystallinity. Detailed studies of the crystallinity of various polyanilines have been reported recently.[30,31] The variation of the crystallinity has been known to be affected by the synthetic methods, substitution, protonation doping, redox processes, and solvent casting. X-ray diffraction measurements were carried out for the N-alkylated polyanilines film samples that were cast from THF solutions without any further thermal treatment.

The X-ray diffractions of N-alkylated polyaniline derivatives are illustrated in Figures 5 and 6 but do not include butylated and octylated polymers, but whose results are plotted in Figure 7. Most of the polymers exhibited broad amorphous scattering around 19° with no discernible order. Other diffused scattering peaks are observed in all samples except PANi-18 at the small angle region 2–6°. This peak with the interplanar spacing depending on the carbon number of the alkyl

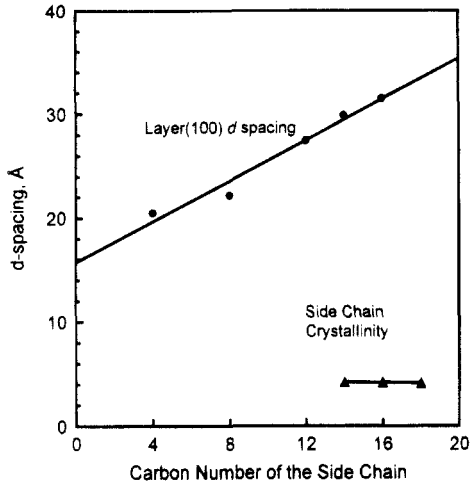

Figure 7. Layer d spacings of N-alkylated PANi as a function of the number of carbon atoms in the side chains.

group can be attributed to a distance between adjacent backbones separated by the side chains in a layered structure.[32] A linear relationship between the Bragg spacing d and the length of the side chains in terms of the number of C atom is depicted in Figure 7. Instead of the 1.25 Å increment of d spacing per CH_2 unit reported for the side chains protruding nearly perpendicular from the main chain,[33] the layer d spacing increment is reduced to 1.0 Å per CH_2 unit in this case. This translates into an increase of the tilt angle of the side chains to the layer planes. The diffusion and the absence of the second- and third-order reflections indicate a weakly defined packing of the main chain as reported for stiff polyesters with flexible side chains by Kricheldorf and Ballauff.[34] The comparison of theoretical values calculated for fully extended side chains in *all-trans* conformation with the experimental d spacings suggests the interdigitation of the side chains. The relatively high intensity of the layer reflections in dodecylated and tetradecylated polyanilines implies that a longer alkyl chain can provide higher free volume for the arrangement of polymer main chains, but not in hexadecylated and octadecylated polymers as explained later. The value 16 Å for the diameter of the polymer backbone from extrapolation of the straight line in Figure 7 to $n = 0$ carbon number also suggests that these polymer main chains may form more complicated layers[35] or unique conformations of main chain because the estimated diameter of the aniline backbone from the geometric structure of aniline is <10 Å.

In the WAXD patterns of the hexadecylated and octadecylated materials, there is a strong and sharp peak at 4.1 Å which overlaps with the wide amorphous halo. The diffraction originates from the side-chain crystalline structure as studied extensively for comblike polymers, such as poly(n-alkyl acrylate)s and poly(N-alkyl acryl amide)s.[36] Studies based on n-paraffins suggest that the side chains of these polymers are in an effort to come into contact with one another, form a packing which averages to a hexagonal lattice whose axes are spaced by 4.1 Å. The hexagonal packing of the alkyl chains in the alkylated polymers also reflects in their IR spectra. The hexagonal form of the alkyl chains is characterized by an absorption maximum at 725 cm^{-1}, corresponding to the oscillation of the C−H groups of the methylene chains. These experimental results are consistent with our previous results with alkylated

Table 6. Transitions in the DSC Thermograms for Polyaniline and Derivatives and Thermal Degradations in TGA Measurements

	thermal transitions, °C									
	first run							second run		
polymers	T_s	T_c	T_g	T_{LC}	T_m	T_{ck}	T_{dec}	$T_{s'}$	$T_{g'}$	$T_{m'}$
PANi-EB			~150[b]			253	539			
PANi-4			75			216	486		90	
PANi-8			66			233	454		68	
PANi-12d			78			228	496		77	
PANi-12c			64			231	476		67	
PANi-12b			59			225	466		60	
PANi-12a			51			235	457		53	
PDAN			43				456			
PANi-14	52	−7	39		146	230	457	6	45	157
PANi-16	−7/48	−2	nd[c]	82	146		468	9		158
PANi-18	18/37	6	nd[c]	102	144		455	25		155

[a] T_s, melting point of side-chain crystallinity; T_c, temperature of side-chain crystallization; T_{ck}, temperature of cross-linking; T_{dec}, temperature of decomposition for the polymers obtained from TGA measurements with N_2 flowing at heating rate 20 °C/min; $T_{m'}$, melting point of the samples after the first heating−cooling cycle annealed at ambient condition for 48 h. [b] DSC value citated from the literature.[51] [c] nd, not determined.

polythiophenes.[37] In the absence of the small-angle diffraction corresponding to the layered structure for PANi-18, it is believed that the partial crystallinity formed by the alkyl side chain leads to the conformational distortions of the backbone and results in the disordering of the layered structures. The effect of side-chain crystallinity on polymer structure was checked by quenching a PANi-18 film sample from 70 °C in liquid nitrogen to minimize the partial crystallization of the side chains. Consequently, the deep suppression of diffraction peaks at 4.1 Å was observed for the quenched sample as pattern 3 in Figure 6.

Computer simulations for the emeraldine base, poly(*N*-dodecylaniline), and *N*-dodecylated polyaniline, with 50% degree of substitution and a random distribution of substituted units along the backbone, were carried out by using the Cerius program. All of the polymeric molecules after minimization in the energy calculation prefer to organize into helical structures; a "fuzzy" rodlike polymer was built up, with 25 Å pitch distances similar to the molecular model established by Daly et al. fo poly(γ-stearyl-α-L-glutamate).[38] PDAN in computer simulation has the smaller end-to-end distance, indicating the enhanced flexibility from N-substitution.

2. Phase Behaviors by DSC Thermograms. Of major interest in these polyaniline derivatives is the effect of the substitution on the thermal behavior of the polymer. Few reports about the thermal properties of the pristine polyaniline have been previously published with vaguely defined glass transition T_g and cross-linking temperature.[39] In this work, great efforts have been made to determine T_g's and other thermal transitions of the modified polyanilines with short ($n = 4, 8$), medium ($n = 12, 14$), and long ($n = 16, 18$) side chains as summarized in Table 6.

For the polymers with short side chains, such as PANi-4 and PANi-8, two thermal transitions are observed between −60 and +170 °C at 20 °C/min heating as shown in Figure 8. The transitions at 75 °C for PANi-4 and at 65 °C for PANi-8 in the first heating runs exhibit second-order shapes with additional endothermal relaxation. In the subsequent heating, only the second-order upshifts in heat capacity are seen. These transitions are assigned to be the glass transition

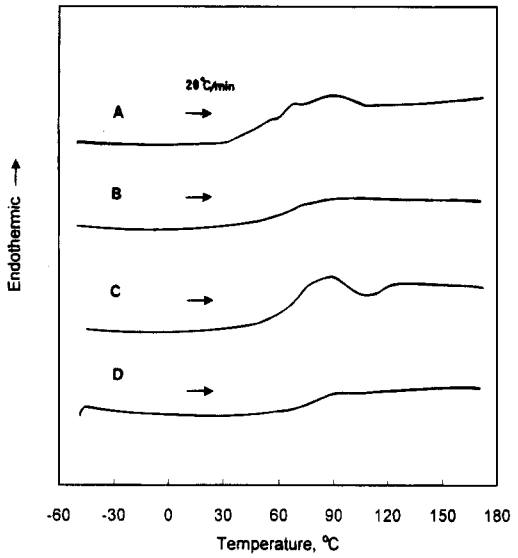

Figure 8. DSC thermograms of PANi-4 in the first heating (A), PANi-4 in the following second heating (B), PANi-8 in the first heating (C), and PANi-8 in the following second heating at the rate of 20 °C/min (D).

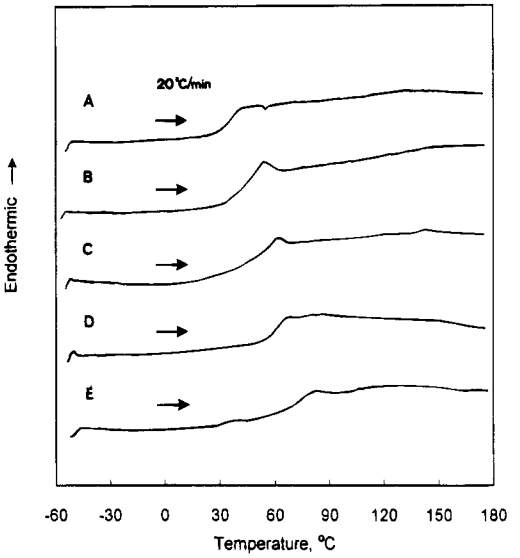

Figure 9. DSC thermograms of PANi-12d (A), PANi-12c (B), PANi-12b (C), PANi-12c (D), and PDAN (E) in the first heating at the rate of 20 °C/min.

temperatures. The observed endothermic heat in the first heating run at the end of the glass transition can be defined as the enthalphic relaxation process of the annealed glassy state.[40] The same observation was also obtained for other conjugated polymers, for instance, poly(alkylthiophene) bearing short side chains.[41] The subsequent second heating runs of the above samples have more distinct second-order glass transitions (90 °C for PANi-4 and 68 °C for PANi-8), almost identical to those values in the first runs. Despite the drastic depression of the glass transitions, the melting point was not observable in the temperature range before the occurrence of cross-linking for these polymers.

By continuous heating, an exothermic transition near 230 °C with an onset at 205 °C is attributed to the cross-linking of the polymers.[39] The samples heated above this temperature were no longer soluble in any organic solvents. More convincing evidence of the cross-linking comes from our temperature-controlled IR data of the N-alkylated polymers upon heating, in which the =N− vibration at 1180 cm^{-1} completely disappears after the sample is heated to 200 °C.

For N-dodecylated polyanilines, the thermal behavior was also investigated in regard to the degree of substitution (Figure 9). The glass transition in the first heating runs is suppressed from 78 °C for the lowest degree of substitution PANi-12d to ~43 °C for the completely substituted PDAN. The second heating runs show identical T_g transitions for these polymers. However, the cross-linking seems to be independent of the degree of substitution and always occurs near 230 °C. Isotropization temperatures were not observed below the cross-linking temperatures. The temperature values of the transitions for the N-dodecylated polymers are summarized in Table 6. The glass transition for PANi-14 is at 45 °C, but for the polyanilines with longer side chains, the detection of glass transition becomes difficult because of the superposition of melting of the side-chain crystals at this temperature region. The influence of the side chain length is clearly presented in a plot of Figure 13, and the decrease in the T_g's seems to be almost linearly dependent on the number of carbons in the side chain. Therefore, it can be concluded

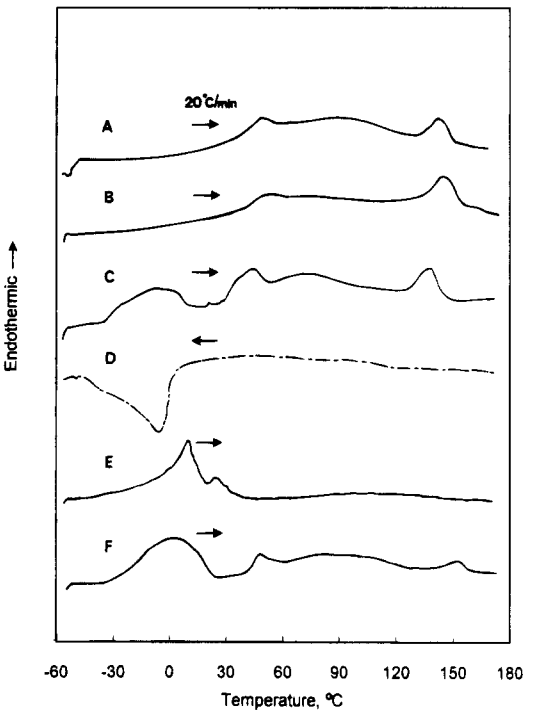

Figure 10. DSC thermograms of PANi-14 in the first heating (A) and the second heating (B) after the former sample annealed at room temperature for 1 week at the rate of 20 °C/min; and PANi-16 in the first heating (C), in the first cooling (D), in the following second heating (E), and in the third heating (F) after the former sample annealed at room temperature for 1 week at the rate of 20 °C/min.

that the solvation effect of the side chains has resulted in depression of the glass transitions.

It is worth mentioning that T_g for the parent polyaniline emeraldine base is estimated from the relationship of T_g values and the size of side chain to be 110−120 °C and is estimated from the dependence of T_g on degree of dodecylation to be 85−100 °C; both of which are much lower than the previously reported values 150−225 °C.[39]

When more than 12 carbons are attached to the backbone, an endotherm appears in the DSC thermograms. Figure 10 shows the thermograms (curves A and B) for PANi-14 referring to first and second heating,

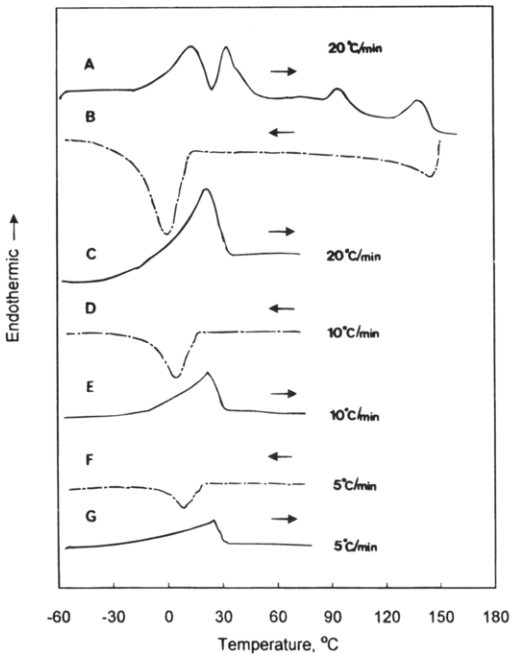

Figure 11. DSC thermograms of PANi-18 in the first heating (A), in the first cooling (B), and in the following second heating (C) at the rate of 20 °C/min; in the second cooling (D) and in the third heating (E) at the rate of 10 °C/min; and in the third cooling (F) and in the fourth heating (G) at the rate of 5 °C/min.

respectively. The upsteps at 39 °C of curve A and 45 °C of curve B were recognized as the glass transitions. No distinct exothermic transitions could be recognized in a cooling run (no curve shown in Figure 10 but included in Table 6 and Figure 13) from 170 °C with the rate even as slow as 2.5 °C/min. Furthermore, the endothermic peak at 156 °C does not exist in the subsequent heating run, but reappears after annealing the sample for at least 48 h at 30 °C. This phenomenon implies that the structural recovery, in particular the orientation of the polymer chains, is very slow and explains why exotherms for any order formations were not observed in the cooling process. This endotherm has been identified as isotropization with the help of observation under optical microscopy. The isotropization transitions are also detected for both PANi-16 (curves C and F in Figure 10) and PANi-18 (curve A in Figure 11) at the same temperature region. Interestingly, that the isotropization transitions are not much affected by a continuous increase in the length of the side chain more than 12 carbon indicates a certain saturation state for the increased flexibility of the polymer due to the substitution.

Alkylated polymers with side chains of 16 or 18 carbons show crystalline birefringence at room temperature under cross-polarized light as shown by photograph A in Figure 12. Dual endothermal melting transitions (Figures 10 and 11) appear between 0 and 50 °C for PANi-16 and PANi-18 and depend on the thermal history of these samples. This transition can be attributed to the melting of the paraffinic side-chain crystals confirmed by WAXD and IR studies. It is well-known that the side-chain crystallinity can be significantly altered by increasing the length of a side chain, the rigidity of the polymer chain, and thermal history. For PANi-16 in curve C of Figure 10, the first broad peak appears at 3 °C and the second peak appears at 48 °C. In the following cooling (curve D in Figure 10), an exothermal transition at −2 °C reflects the crystallization

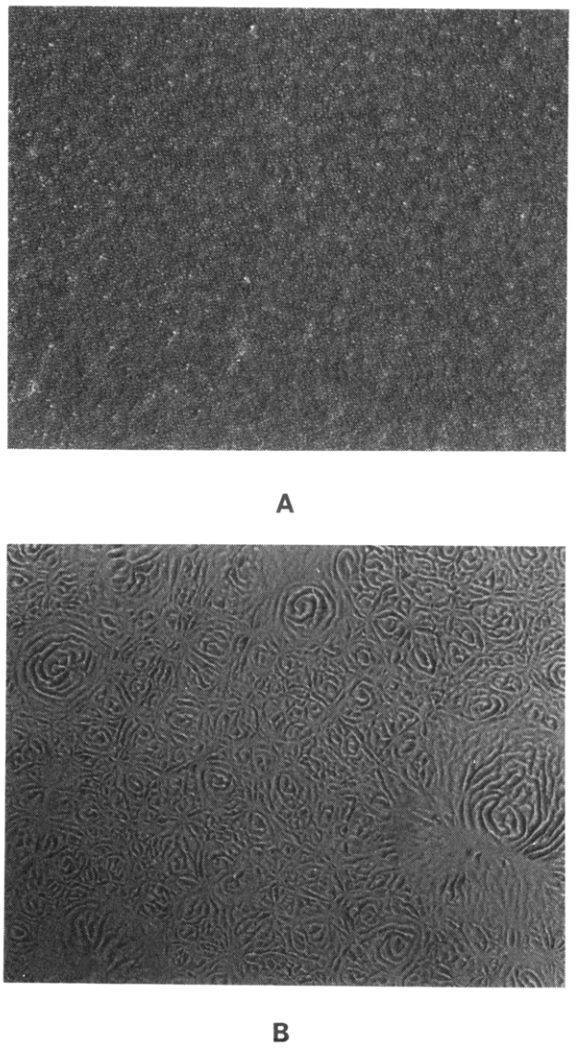

Figure 12. Optical microscopic photographs for PANi-18 at room temperature (A) and heated to 65 °C (B).

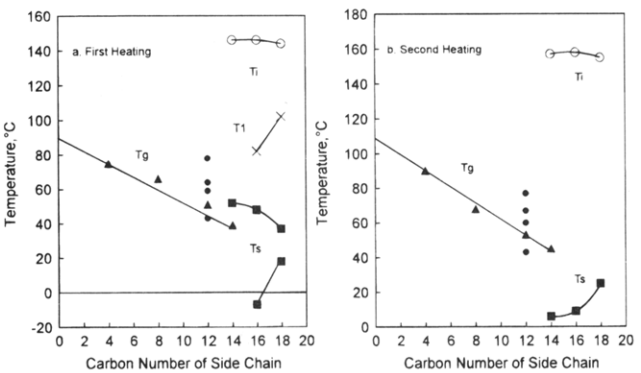

Figure 13. Phase diagrams of N-alkylated polyanilines: (a) the first runs; (b) the second runs. (△) T_g for the polymers with different size of side chains; (●) T_g for the polymers with various degree of alkylation; (■) T_s melting of side chain crystalline; (○) T_i isotropization transition; (×) T_1 mesophase Transition.

of alkyl side chains. Only one endotherm appears at 27 °C in the subsequent heating (curve E of Figure 10) after 20 °C/min cooling below −60 °C. For PANi-18 in curve A of Figure 11, the two peaks located 18 and 37 °C, respectively. The temperature of side-chain crystallization in the subsequent cooling is located at 6 °C. After the first heating−cooling cycle (between −60 and +170 °C), the second heating (curve C in Figure 11) only showed one peak at 25 °C. It is suggested that two

melting behaviors ascribed to the side-chain crystallinities resulting from the different crystallization processes and that they vary appreciably with the sample treatment.[16,42] The higher melting point T_{s2} may correspond to the tight crystallinities with a high degree of interdigitation. After the fast quench from melt, the distribution of crystallities (PANi-16 curve E in Figure 10) is not bimodal but broad, and finally, after a slow cooling a well-defined sharp melting near 50 °C is observed (curve F). The consequence is the same for PANi-18 after the same thermal treatment (no curve shown and covered by Table 6 and Figure 13).

The cooling and heating processes were repeated at various scanning rates (20−5 °C/min) in the range of −60 to +70 °C for PANi-18 in order to investigate the side-chain crystallinity. A repeating "annealing" process at 70 °C will maximize the layering. Only one endothermic transition at 18 °C was observed in the following heating and one exothermic peak at 2.5 °C in the following cooling independent of the cooling rate. But the heat of melting ΔH_s and the heat of crystallization ΔH_{cs} integrated from DSC transition peaks are dependent on the scanning rates, indicating that the side-chain crystallization is sensitive to its thermal history.[43] As seen in Figure 11, the general feature is that side-chain crystallization decreases with the annealing process. Interestingly, a long-time annealing at 30 °C can induce well-formed crystals with high melting point by the side chains. The long-time annealing of the above sample at 30 °C resulted in one DSC peak at 48 °C in curve F of Figure 10 consistent with an increase in side-chain crystallinity as shown X-ray diffraction pattern 4 in Figure 6. Also pattern 3 illustrated in Figure 6 with a weaker peak at 4.1 Å supports this view.

The presence of long aliphatic side chains may promote the formation of thermotropic liquid crystals.[7,37,44] In principle, the rigid polymer blocks could perform as mesogenic units connected with alkyl side chains as flexible spaces, and the formation of a thermotropic liquid crystalline phase with the increase in temperature should occur as a result of the cooperative motion of these segments. When the alkyl side chains reach a critical length, the polymer may even form thermotropic liquid crystals above the melting point of the side chain. These new types of liquid crystalline polymers were suggested to be different from the classic main-chain and side-chain liquid crystal polymers, called "fuzzy" rigid-rod LCP. Such thermotropic liquid crystalline polymers including poly(γ-alkyl aryl-α L-glutamate)s and some rigid-rod polyesters with flexible side chains have been reported.[7,38]

The additional transitions in the middle-temperature region were detected by DSC runs in curve C of Figure 10 for PANi-16 and in curve A of Figure 11 for PANi-18. The transitions were observed at 84 °C for PANi-16 with an associated enthalpy of 2.7 J/g and at 102 °C for PANi-18 with 4.0 J/g. Optical microscopy was utilized to assist the determination of the complicate phase behaviors of PANi-16 and PANi-18. Thin films were cast from THF solutions on the glass slides and slowly heated at a rate of 5 °C/min under optical microscopy. At room temperature, both samples showed crystalline birefringence under polarized light. It was found that a highly viscous fluid with a texture physical of a thermotropic liquid crystalline phase was formed when the samples were heated to a temperature above T_s melting of the side-chain crystallites. A photograph

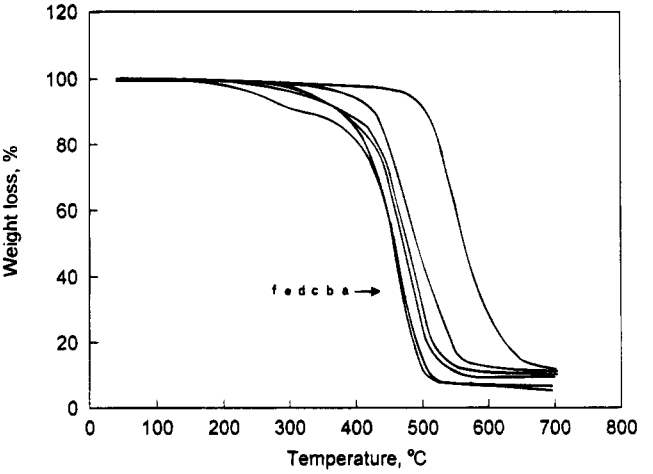

Figure 14. Thermogravimetric runs of PANi-EB powder (a), PANi-12d (b), PANi-12c (c), PANi-12b (d), PANi-12a (e), and PDAN (f) under purge of N_2 gas at a heating rate of 20 °C/min.

taken of the heated PANi-18 is presented in Figure 12B. The phenomenon indicates the presence of a liquid crystalline mesophase. The endothermal transitions in PANi-16 and PANi-18 can be interpreted as a transformation from one mesophase to another. After melting of the paraffinic side-chain crystallinities, polymer chains still adopt the local layered structure but the disordering of the side chains induces mobility between layers.[42,43] This lubrication effect decreases the three-dimensional ordering of the layers. It has been suggested that the second mesophase is more complicated and no long-range translational order was detectable in this mesophase by WAXD data in the work of Watanabe et al.[7] It is highly propable that the second transition involves a smectic to a nematic type of transition, resulting in a state in which the orientation of chains is still preserved but no axial correlation exists between the neighboring chains.

3. Thermostability. Figure 14 shows the thermogravimetric measurements in a nitrogen atmosphere of the emeraldine base, N-dodecylated polyanilines at various alkylation levels, and fully alkylated PDAN. The three peaks in the derivative plots of the substituted polymers and two peaks of emeraldine indicated the possible multiple steps of decomposition. The minor weight loss (<5%) at a low-temperature range in some samples should be attributed to little water or solvent trapped in the polymers. The substituted polymers actually undergo two competing degradation steps, clearly described by the two overlapped peaks in the derivative plots. The temperatures of maximum degradation in two extreme cases, fully substitued PDAN and unsubstituted PANi-EB, locate at 456 and 540 °C, respectively. For partially alkylated polymers, a slow degradation step occured with the onset at 300 °C, and a second sharp degradation step followed with the completion of weight loss by 650 °C. The ratio of the weight loss in the two competitive steps varied with the degree of alkylation. Obviously, the tertiary aromatic amines substituted by alkyl groups had less thermal stability than a secondary amine.[45]

At 650 °C with complete degradation, the amount of residue remaining is propotional to the percentage of the secondary amine substitued by alkyl groups. Interestingly, the polymers with a side chain longer than the butyl group exhibited thermal stability independent of the length of the side chain.

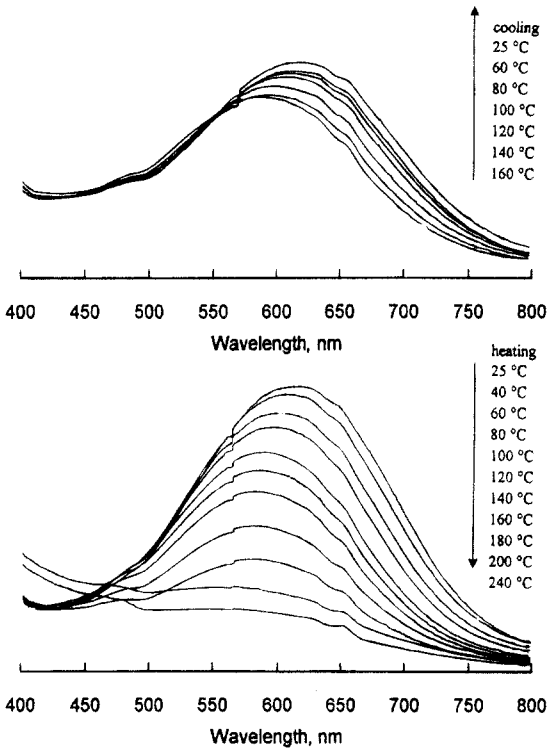

Figure 15. UV–visible spectra and thermochromic effects in N-octylated polyaniline.

4. Thermochromism in Solid State. In addition to the solution properties in the neutral state, these polyaniline derivatives also exhibit interesting reversible thermochromic effects. Similar properties have been reported widely for poly(3-alkylthiophene),[46,47] polydiacetylene,[48] and polysilanes,[48] in which the thermochromism is attributed to conformational transtions of the polymer chain from a coplanar structure to a nonplanar structure. The side chains assist the formation of planarity, as the maximum planarity has been reached with 12 carbons for PAT. However, as mentioned above, polyanilines in the neutral states have been proved not to have a coplanar conformation as polythiophene and polypyrrole. The phenyl ring of the polyaniline backbone is twisted at an angle ϕ out of the C–N–C plane.[1] The conjugation along a aniline backbone is correlated with the degree of orbital overlap between the phenyl π electrons and the nitrogen sp^3, directly dependent on the torsion angle ϕ between the phenyl plane and the C–N–C plane.

Therefore, in order to gain insight into the influence of the substitution pattern on conformation and conjugation, the temperature dependence of the optical absorption spectra of the various alkyl-substituted polyanilines has been measured. Figure 15 shows that UV-visible absorption spectra of PANi-8 obtained upon heating from 25 to 240 °C and cooling from 160 to 25 °C. At room temperature, a transparent thin film of PANi-8 cast from THF solution exhibits two absorptions at 622 and 300–330 nm. Because the latter maximum absorption is difficult to identify, only the absorption at the relatively long wavelength 622 nm (~2 eV) was monitored upon heating or cooling. Upon heating, the color of the sample (actual color shift was monitored by optical microscopy without filtration lens) shifts continuously from blue, 622 nm, at room temperature, to purple, 584 nm, at 160 °C, to yellow without a distinguished absorption near 600 nm at 200 °C, and to orange with a shoulderpeak 480 nm at 240 °C. The process is reversible if heating is stopped below 160 °C. Furthermore, there is no evidence of coexistence of two different phases in this case as obtained in poly(3-alkylthiophene),[49] and the change in the absorption maxima is continuous under our experimental conditions.

The temperature dependences of UV–visible absorptions of PANi-12a and -b, PANi-14, and PANi-16 display patterns similar to that of PANi-8 described above. The upper limit temperatures of these samples for reversible optical behavior are 160, 160, and 120 °C, respectively. In correlation with the DSC thermal transitions, it is clear that the significant color change observed near 160 °C is related to the isotropization of the polymer chains for PANi-14 and PANi-16 samples.

According to the previously discussed optical properties in solution state, the interchain interactions have very little influence on the conformational structures of an isolated polymer chain. However, the intrachain steric interaction may be dominant to twist an individual polymer chain in the solution state because the conjugation of the backbone is somewhat dependent on the situation of the substituents. As reported in Table 4, at room temperature, the N-substituted polyanilines exhibit a maximum of absorption in the solid state with a red shift of 5–10 nm from the maximum of absorption in solution, as mentioned in the previous section on optical properties. More factors should be considered to affect the optical properties of conjugated polymers bearing flexible side chains in the solid state, including strong interchain electronic interactions, possible anisotropic packing in three dimensions, and orientational phases of the main chains or side chains. These factors vary with the temperature. Therefore, the conformation of packed polymer chains in the solid state will be determined by the free volume brought up by the side chains and the entropy provided by the increase of temperature accompanied with phase transitions.

In contrast, PANi-4 and PANi-18 samples did not exhibit thermochromic effects similar to the PANi-8. During the heating processes, PANi-4 might not adopt the conformational changes due to the tight free volume provided by short side groups, while during the cooling process, PANi-18 with long side chains undergoes side-chain crystallization, distorting the layer formation.

The temperature-dependent infrared spectra of alkylated polymers provided the decisive evidence for the conformational change of the polymer chains associated with thermochromic shifts in the UV–visible absorption. The infrared spectra indicate the side chains experience conformational disordering upon heating. More important information about polymer conformational changes can be obtained from the temperature dependence of the vibrational motions related to the polymeric backbone. The IR absorption bands of the quinoid form do not remain at high temperature and become weaker rapidly above 160 °C. A similar observation is found for the absorption of =N– vibration, which almost completely disappears at 200 °C because cross-linking takes place.

The temperature-dependent UV–visible absorptions and FT-IR analyses of the alkylated polymers have revealed that disorder is created in both the main chain and side chain upon heating. When compared to poly(alkylthiophenes), the cooperative effect of the twisting of backbone units and disordering of the substituents is inhibited by the rigid quinoid form showing that poly-

(alkylanilines) maintain rigidity better after substitution. The thermochromic behavior of N-alkylated polyanilines in the solid state (alkyl side chains serve as bound solvent) is analogous to that of EB in NMP solvent investigated by Epstein et al.[50,51] Both optical absorptions at 3.8 and 2.0 eV shift to higher energy and weaken with increase in temperature due to the rise in thermal expansion of the average phenyl ring−torsion angles and to the constant reduction in the band width and average energy of the valence band. Our results not only support these concepts but also show that the process occurs easier and reversibly in our N-alkylated samples. Further, the cooperative disordering process also results in a stable processable temperature region in addition to the possible formations of liquid crystalline and side-chain crystalline phases.

Conclusion

In the present paper, we have demonstrated that the incorporation of alkyl substituents in various sizes may be applied for polyaniline leucoemeraldine to control the chemical structure, to innovate in its tractability for processing application, and to modify the physical properties of this conjugated polymer. The NMR and FT-IR spectroscopy and elemental analysis study have been helpful in characterization of the model compound and its derivatives as well as a series of alkylated polyaniline derivatives. The solubility is improved remarkably in common organic solvents (chloroform, tetrahydrofuran, toluene, etc.) for products with more than eight carbons on the side chain and ~38% alkylation of the reactive nitrogen sites. The neutral polyaniline derivatives exhibit interesting solvatochromic and thermochromic phenomena, which are believed to be related to a conformational change induced by the interaction of the aniline backbone in different solvent environments and the cooperative twisting of repeat units combined with disorder of the side chains upon heating. The alkylated polyanilines exhibit interesting thermal and morphological properties in the bulk state. The alkyl substitution induces the layered structure wherein the interlayer d spacing of alkyl side-chain interdigitation between two adjacent stacks of polymer chains is sensitive to its effective length. In addition, the morphology was found to be altered in polymers (PANi-16 and PANi-18) with long side chains ($n > 14$) since the interdigitation of side chains is sufficiently well-defined to form a crystalline phase. The glass transition temperature has been correlated with the degree of alkylation and length of side chain, and the extrapolated T_g for the pristine polyaniline (PANi-EB) is ~100 °C. Some polymers display isotropization transitions at lower temperatures before cross-linking if the alkyl side chains are sufficiently long and concentrated. The long alkyl side chains facilitate the formation and transformation of mesophases by functioning as flexible spacers to decouple individual mesogenic units from entire polymer chains. The role of solvent assumed by the flexible side chains on liquid crystalline behavior of conjugated polymers will be investigated in detail in our future work. Study of these processable polyanilines has been expanded to their structure and properties in the doped state and to the miscibility of their blends with flexible polymers these will be covered in our upcoming papers.[52]

References and Notes

(1) Genies, E. M.; Boyle, A.; Lapkowski, M.; Tsintavis, C. *Synth. Met.* **1990**, *36*, 139.
(2) MacDiarmid, A. G.; Chiang, J. C.; Epstein, A. J. *Faraday Discuss. Chem. Soc.* **1989**, *88*, 317.
(3) Sugimoto, R.; Takeda, S.; Gu, H. B.; Yoshino, K. *Chem. Express* **1986**, *1*, 635.
(4) Sato, M. A.; Tanaka, S.; Kaeriyama, K. *J. Chem. Soc., Chem. Commun.* **1986**, 873.
(5) Yoshino, K.; Park, S. H.; Sugimoto, R. *Jpn. J. Appl. Phys.* **1988**, *27*, L716.
(6) Stern, R.; Ballauff, M.; Wegner, G. *Makromol. Chem., Makromol. Symp.* **1989**, *23*, 373.
(7) Watanabe, J.; Harkness, B. R.; Sone, M.; Ichimura, H. *Macromolecules* **1994**, *27*, 507.
(8) Plate, N. A.; Shibaev, V. P. *Comb-Shaped Polymers and Liquid Crystals*; Plenum Press: New York, 1987; Chapter 1.
(9) Chevalier, J. W.; Bergeron, J. Y.; Dao, Lê H. *Macromolecules* **1992**, *25*, 3325.
(10) Wei, Y.; Focke, W. W.; Wnek, G. E.; Ray, A.; MacDiarmid, A. G. *J. Phys. Chem.* **1989**, *93*, 495.
(11) Leclerc, M.; Guay, J.; Dao, L. H. *Macromolecules* **1989**, *22*, 649.
(12) Bergeron, J. Y.; Chevalier, J. W.; Dao, L. H. *J. Chem. Soc., Chem. Commun.* **1990**, 180.
(13) Takayanagi, M.; Katayose, T. *J. Polym. Chem. Ed.* **1981**, *19*, 1133.
(14) Kim, Y. H.; Calabrese, J. C. *Macromolecules* **1991**, *24*, 2951.
(15) Hagiwara, T.; Yamaura, M.; Iwata, K. *Synth. Met.* **1988**, *26*, 195.
(16) Takayanagi, M.; Katayose, T. *J. Appl. Polym. Sci.* **1984**, *29*, 141.
(17) Ni, S.; Tang, J.; Wang, F.; Shen, L. *Polymer* **1992**, *33*, 3607.
(18) Kenwright, A. M.; Feast, W. J.; Adams, P.; Milton, A. J.; Monkman, A. P.; Say, B. J. *Synth. Met.* **1993**, *55−57*, 666.
(19) Furukawa, Y.; Ueda, F.; Hyodo, Y.; Harada, I.; Nakajima, T.; Kawagone, T. *Macromolecules* **1988**, *21*, 1297.
(20) Aiba, S. *Makromol. Chem.* **1993**, *194*, 65.
(21) Wei, Y.; Hsueh, K. F.; Jang, G. W. *Macromolecules* **1994**, *27*, 518.
(22) Roughooputh, S. D. D. V.; Hotta, S.; Heeger, A.; Wudl, F. *J. Polym. Sci., Polym. Phys. Ed.* **1987**, *25*, 1071.
(23) Roux, C.; Faïd, K.; Leclerc, M. *Polym. News* **1994**, *19*, 6.
(24) Huang, W. S.; MacDiarmid, A. G. *Polymer* **1993**, *34*, 1833.
(25) Barbero, C.; Miras, M. C.; Haas, O.; Kötz, R. *J. Electroanal. Chem.* **1991**, *310*, 437.
(26) Levon, K.; Ho, K.-S.; Laakso, J.; Mao, J.; Zheng, W.-Y. *Synth. Met.* **1993**, *55−57*, 3591.
(27) Ghosh, S.; Kalpagam, V. *Synth. Met.* **1989**, *33*, 11.
(28) Yue, J.; Wang, Z. H.; Cromack, K. R.; Epstein, A. J.; MacDiarmid, A. G. *J. Am. Chem. Soc.* **1991**, *113*, 2665.
(29) Oka, O.; Kiyohara, O.; Yoshino, K. *Jpn. J. Appl. Phys.* **1991**, *30*, L653.
(30) Laridjani, M.; Pouget, J. P.; Scherr, E. M.; MacDiarmid, A. G.; Jozefowicz, M. E.; Epstein, A. J. *Macromolecules* **1992**, *25*, 4106.
(31) Pouget, J. P.; Józefowicz, M. E.; Epstein, A. J.; Tang, X.; MacDiarmid, A. G. *Macromolecules* **1991**, *24*, 779.
(32) Prosa, T. J.; Winokur, M. J.; Moulton, J.; Smith, P.; Heeger, A. J. *Macromolecules* **1992**, *25*, 4364.
(33) Ho, K.-S.; Laakso, J.; Levon, K.; Mao, J.; Taka, T.; Zheng, W.-Y. *Synth. Met.* **1993**, *55−57*, 384.
(34) Cervinka, L.; Ballauff, M. *Colloid Polym. Sci.* **1992**, *270*, 859.
(35) Kricheldorf, H. R.; Schwarz, G.; Domschke, A.; Linzer, V. *Macromolecules* **1993**, *26*, 5161.
(36) Sobottka, I.; Sochava, I. V. *Vysokomol. Soyed.* **1979**, *A21*, 1322.
(37) Hsu, W. P.; Levon, K.; Ho, K. S.; Myerson, A. S.; Kwei, T. K. *Macromolecules* **1993**, *26*, 1318.
(38) Daly, W. H.; Poché, D.; Negulessu, I. I. *Prog. Polym. Sci.* **1994**, *19*, 79.
(39) Wei, Yen; Jang, G. W.; Hsueh, K. F.; Scherr, E. M.; MacDiarmid, Epstein, A. J. *Polymer* **1992**, *33*, 314.
(40) Bosma, M.; Brinke, G.; Ellis, T. S. *Macromolecules* **1988**, *21*, 1465.
(41) Chen, S. A.; Ni, J. M. *Macromolecules* **1992**, *25*, 6081.
(42) Rubin, I. D. *J. Appl. Poly. Sci.* **1988**, *36*, 445.
(43) Kunisada, H.; Yuki, Y.; Kondo, S.; Igarashi, H. *Polymer* **1991**, *32*, 2283.
(44) Qian, R.; Chen, S.; Song, W.; Bi, X. *Macromol. Rapid Commun.* **1994**, *15*, 1.
(45) Kang, E. T.; Neoh, K. G.; Tan, T. C.; Khor, S. H.; Tan, K. L. *Macromolecules* **1990**, *23*, 2918.
(46) Roux, C.; Leclerc, M. *Macromolecules* **1992**, *25*, 2141.

(47) Tashiro, K.; Minagawa, Y.; Kobashi, M.; Morita, S.; Kawai, T.; Yoshino, K. *Synth. Met.* **1993**, *55–57*, 321.
(48) Yuan, C. H.; West, R. *Macromolecules* **1994**, *27*, 629.
(49) Pei, Q.; Järvinen, H.; Österholm, J. E.; Ingänas, O.; Laakso, J. *Macromolecules* **1992**, *25*, 4297.
(50) Master, J. G.; Ginder, J. M.; MacDiarmid, A. G.; Epstein, A. J. *J. Chem. Phys.* **1992**, *96*, 4768.
(51) Ginder, J. M.; Epstein, A. J. *Phys. Rev. B* **1990**, *41*, 10674.
(52) Zheng, W. Y.; Levon, K.; Taka, T.; Laakso, J.; Österholm, J., manuscript in progress.